Proton stopping power of aluminum ions

E. J. McGuire, J. M. Peek, and L. C. Pitchford
Sandia National Laboratories, Albuquerque, New Mexico 87185
(Received 20 November 1981)

With the use of the generalized-oscillator-strength formulation of the plane-wave Born approximation, the contribution of individual subshell ionization and excitation to the proton stopping power is calculated for Al^{n+} $(0 \leq n \leq 11)$ for proton energies between 0.1 and 100 MeV. The neutral-Al results are in excellent agreement with experiment. The subshell-peak stopping power due to ionization is in excellent agreement with scaled neutral-atom values. The optical oscillator strength was used to calculate the Bethe mean-excitation energy I for all the Al ions. Equating the explicitly calculated stopping power at 100 MeV to the Bethe formula led to an alternative I value. While the two I values agreed for some ions, for others they disagreed by as much as 50%. However, even in such cases, a change of less than 10% in the stopping power at 100 MeV would produce agreement between the two methods of calculating I.

I. INTRODUCTION

Currently Al is being used as a target material in the light-ion beam fusion program,[1] and has been used in laser matter-interaction studies.[2,3] In the latter case the plasma temperature is high (several hundred eV) and radiation from hydrogenic and heliumlike Al provides a useful diagnostic. Plasma temperatures in the light-ion beam targets are low (tens of eV) and radiation diagnostics are most complex. In addition, the light-ion beam (hereinafter protons) heating of the Al target is a complex process, as the energy deposition in both ions and free electrons is temperature dependent. The need for reliable Al-ion stopping powers is the motivation for these calculations.

Our approach[4,5] to ionic stopping-power calculations is to calculate explicitly the contribution to the stopping power of excitation and ionization of each occupied subshell in as efficient a manner as possible. The technique used is the generalized-oscillator-strength (GOS) formulation of the Born approximation using one-electron orbitals found from the Schrödinger equation with a central potential obtained from a piecewise continuous approximation to $[-rV(r)]$ of Herman and Skillman.[6] As a check on the applicability of the Born approximation and the central potential employed, we have used our Al-ion GOS to calculate electron ionization cross sections.[7] These are in reasonable agreement with other calculations and measurements except, as expected, near threshold.

Because there are a small number of Al ions and a small number of occupied subshells per ion, GOS calculations were performed for all occupied subshells. This is in contrast to our calculations on stopping power for gold ions,[5] where for deep inner shells the ionization contribution to stopping power is calculated via scaling laws, and the excitation contribution from deep inner shells is neglected. With the complete set of Al-ion GOS, the Bethe[8] mean-excitation energy I can be explicitly calculated and compared with an I value inferred from fitting a Bethe formula to the explicity calculated stopping power. A comparison of the two I values illuminates the validity of the calculations.

In Sec. II we sketch the computational procedure, discuss the approximations that are significant at high energy, and present the results of the explicit calculations (to 100 MeV). In Sec. III we present the sum-rule calculation of the Bethe mean-excitation energy I and compare it with values inferred from the explicit calculations.

II. EXPLICIT CALCULATIONS.

The one-electron GOS to the continuum per nl electron per $\epsilon l'$ continuum hole is defined by[8]

$$\frac{df_{nl}}{d\epsilon}(\epsilon,K^2,l')=\frac{\Delta E}{K^2}\,|\,\langle nl\,|\,e^{i\vec{K}\cdot\vec{r}}\,|\,\epsilon l'\rangle\,|^2\,, \tag{1}$$

where $\Delta E=\epsilon-E_{nl}$ is in Ry (13.6 eV), $-E_{nl}$ is the one-electron ionization energy of the nl subshell, ϵ is the continuum electron energy with $\epsilon=0$ at the ionization threshold, r is the magnitude of the electron position vector in Bohr radii, K is the magni-

tude of the momentum transfer in inverse Bohr radii, and $df/d\epsilon$ is in Ry^{-1}. Expanding the exponential in Eq. (1) in Legendre polynomials and Bessel functions leads to explicit expressions for the subshell GOS. For $l=0,1,2$ the expressions are given in Ref. 9. The orbitals used in the calculations were obtained by first approximating the quantity $[-rV(r)]$ of Herman and Skillman[6] by a series of straight lines (up to six for Al ions), and then solving the Schrödinger equation with the derived potential. This Schrödinger equation is exactly solvable in terms of Whittaker functions permitting the relatively rapid generation of properly normalized continuum orbitals.

The contribution of subshell ionization to the stopping power is given by

$$S_{nl}^{c}=\frac{4\pi a_0^2}{(M_e/M_p)E_p}Z_{nl}\times\int_0^{E_p-E_{nl}}d\epsilon\int_{K^2_{\min}}^{K^2_{\max}}\frac{dK^2}{K^2}\sum_{l'=0}^{\infty}\frac{df_{nl}}{d\epsilon}(\epsilon,K^2,l')\,, \tag{2}$$

where E_p is the proton energy in Ry, a_0 is the Bohr radius, M_e and M_p are the electron and proton masses, respectively, Z_{nl} is the number of electrons in the nl subshell, and

$$K^2_{\substack{\max\\ \min}}=\frac{M_p}{M_e}(\sqrt{E_p}\pm\sqrt{E_p-\epsilon-E_{nl}})^2\,.$$

For the excitation contribution to the stopping power S_{nl}^{D} ones uses $\Delta E=E_{n'l'}-E_{nl}$ in Eq. (1) and drops the integral over ϵ in Eq. (2). The excited orbitals included all those up to $n'\leq 5$ and $l'=0,1,2$.

There is an infinite sum over l' in Eq. (2). In these calculations the sum was limited to $l'\leq 12$. The integration over r in Eq. (1) was done on a 200-point grid extending up to $R_{\max}$, where $\varphi(R_{\max})\leq 10^{-4}\varphi(R)_{\max}$ (essentially the cutoff criterion in Herman and Skillman[6]). For accuracy in the calculated GOS, ϵ was limited by $\sqrt{\epsilon}\Delta R\leq\pi/5$, where $\Delta R=R_{\max}/200$. This criterion typically truncated our GOS grid at $\epsilon\approx 50E_{nl}$. The upper limit of K^2 in the grid (K_u^2), was always larger, i.e., $K_u^2>50E_{nl}$, allowing us to obtain an asymptotic expression in K^2 for $\epsilon\leq 50E_{nl}$. The region $K^2>50E_{nl}$, $\epsilon\leq 50E_{nl}$ is of little significance except at very-low-incident proton energies, where ionization cross sections and stopping-power contributions are small, and not well calculated by the Born approximation.

For $\epsilon\geq 50E_{nl}$ (the region where the Bethe ridge dominates the GOS), the GOS was written[4] as $Z_{nl}\delta(\epsilon-K^2)$ for $K^2\geq 50E_{nl}$. Z_{nl} was chosen to be the number of electrons in the subshell. This delta-function approximation adds a term of the form[4]

$$\frac{4\pi a_0^2 Z_{nl}}{(M_e/M_p)E_p}\ln(4M_eE_p/M_pNE_{nl})\times\Theta(E_p-NE_{nl}M_p/4M_e) \tag{3}$$

to the stopping power, where NE_{nl} is the secondary electron energy at which explicit GOS calculations are truncated.

For $\epsilon\geq 50E_{nl}$ and $K^2\leq 50E_{nl}$, where the GOS is small but not negligible, an asymptotic expression was employed. The integral over momentum transfer in Eq. (2) leads to a function $dS_{nl}/d\epsilon(E_p,\epsilon)$. From the two largest ϵ values used in the calculation an asymptotic contribution to the subshell stopping power was obtained. This asymptotic contribution could be as much as 10% of the subshell stopping power. Corrections of this size are important in determining the Bethe mean-excitation energy from the explicit stopping-power calculations as I is determined by exponentiating the calculated stopping power.

In Table I the calculated stopping power S_T, including both excitation S_D and ionization S_c is listed for Al^{q+} with $0\leq q\leq 11$ for proton energies from 0.1 to 100 MeV. Table II are lists of the ionization and excitation contributions from each subshell of neutral Al at 10 and 100 MeV. Table II shows the "unimportance" of inner-shell excitation and the dominance of 3s subshell excitation. This arises from the $(3s)^2(3p)$-$(3s)(3p)^2$ transition. The relatively large contribution of resonance transitions to stopping power, even though the energy lost in the transition is small, has been noted earlier.[4] The neutral-Al stopping power is prorated in the row labeled Z^* in Table II. Even at 100 MeV the three outermost subshells contribute more to stopping power than a naive application of the Bethe formula would suggest. The last two rows in Table II list the summed optical oscillator strengths for the various neutral-Al subshells from our calculations and those of Dehmer *et al.*[10] While both sets of $\sum f$ show a pattern qualitatively similar to Z^*, quantitatively there are substantial differences, e.g., the continuum (discrete) contribution to $\sum f$ for the 3s subshell is 0.315 (1.516), while the 3s continuum (discrete) contribution to Z^* is 1.43 (1.04) at 100 MeV.

In an earlier paper[4] one of us advanced a scaling hypothesis for the ionization contribution to subshell stopping power, i.e., S_{nl}^{C} can be written as

TABLE I. The calculated continuum, discrete, and total stopping power (in 10^{-15} eV cm^2) for Al^{n+} ($0 \leq n \leq 11$) for protons with energy between 0.1 and 100 MeV.

E_p	Al^{0+}			Al^{1+}			Al^{2+}			Al^{3+}			Al^{4+}		
(MeV)	S_c	S_D	S_T	S_c	S_D	S_T	S_c	S_D	S_T	S_c	S_D	S_T	S_c	S_D	S_T
0.1	14.2	8.8	23.0	6.98	8.97	16.0	3.89	4.77	8.66	1.89	0.86	2.75	1.12	1.21	2.33
0.2	16.7	5.3	16.0	6.67	5.35	12.0	4.57	2.98	7.55	3.06	0.82	3.88	2.07	1.14	3.21
0.3	9.37	3.92	13.3	6.34	3.90	10.2	4.74	2.24	6.98	3.52	0.73	4.25	2.49	1.02	3.51
0.4	8.44	3.13	11.6	5.97	3.10	9.07	4.65	1.81	6.46	3.63	0.66	4.29	2.65	0.92	3.57
0.5	7.85	2.63	10.5	5.61	2.59	8.20	4.49	1.53	6.02	3.59	0.60	4.19	2.67	0.84	3.51
0.6	7.34	2.27	9.61	5.28	2.24	7.52	4.30	1.34	5.64	3.50	0.55	4.05	2.62	0.77	3.39
0.7	6.88	2.01	8.89	5.01	1.97	6.98	4.11	1.19	5.30	3.38	0.51	3.89	2.56	0.71	3.27
0.8	6.46	1.80	8.25	4.77	1.77	6.54	3.94	1.07	5.01	3.26	0.47	3.73	2.47	0.66	3.13
1.0	5.75	1.50	7.25	4.35	1.47	5.82	3.62	0.90	4.52	3.02	0.42	3.44	2.30	0.59	2.89
2.0	3.79	0.84	4.63	2.99	0.82	3.81	2.53	0.52	3.05	2.15	0.27	2.42	1.71	0.39	2.10
3.0	3.09	0.60	3.69	2.51	0.58	3.09	2.05	0.38	2.43	1.69	0.21	1.90	1.46	0.30	1.76
4.0	2.63	0.47	3.10	2.17	0.45	2.62	1.80	0.30	2.10	1.49	0.17	1.66	1.26	0.24	1.50
5.0	2.25	0.39	2.64	1.88	0.37	2.25	1.58	0.25	1.83	1.34	0.15	1.49	1.10	0.21	1.31
6.0	1.97	0.33	2.30	1.66	0.32	1.98	1.40	0.21	1.61	1.20	0.13	1.33	0.983	0.181	1.16
7.0	1.76	0.29	2.05	1.48	0.28	1.76	1.26	0.19	1.45	1.08	0.11	1.19	0.887	0.161	1.05
8.0	1.59	0.26	1.85	1.34	0.25	1.59	1.15	0.17	1.32	0.986	0.103	1.09	0.810	0.146	0.956
10.0	1.34	0.21	1.55	1.14	0.21	1.35	0.974	0.138	1.11	0.841	0.087	0.928	0.692	0.173	0.815
20.0	0.771	0.116	0.887	0.663	0.111	0.774	0.578	0.076	0.654	0.500	0.050	0.550	0.418	0.072	0.490
40.0	0.441	0.063	0.504	0.383	0.060	0.443	0.335	0.042	0.377	0.294	0.029	0.323	0.245	0.041	0.286
70.0	0.275	0.038	0.313	0.240	0.036	0.276	0.211	0.026	0.237	0.186	0.018	0.204	0.155	0.026	0.181
100.0	0.203	0.028	0.231	0.177	0.026	0.203	0.156	0.019	0.175	0.138	0.013	0.151	0.114	0.019	0.133

E_p	Al^{5+}			Al^{6+}			Al^{7+}			Al^{8+}			Al^{9+}		
(MeV)	S_c	S_D	S_T	S_c	S_D	S_T	S_c	S_D	S_T	S_c	S_D	S_T	S_c	S_D	S_T
0.1	0.61	1.32	1.93	0.32	1.40	1.72	0.158	1.40	1.56	0.068	1.38	1.45	0.022	1.35	1.37
0.2	1.29	1.22	2.51	0.80	1.26	2.06	0.465	1.20	1.67	0.255	1.11	1.37	0.124	1.00	1.12
0.3	1.65	1.10	2.75	1.09	1.12	2.21	0.679	1.06	1.74	0.398	0.945	1.34	0.213	0.818	1.03
0.4	1.82	0.99	2.81	1.23	1.01	2.24	0.803	0.945	1.75	0.490	0.834	1.32	0.271	0.702	0.973
0.5	1.89	0.90	2.79	1.31	0.92	2.23	0.866	0.855	1.72	0.543	0.749	1.29	0.307	0.620	0.927
0.6	1.88	0.83	2.71	1.33	0.84	2.17	0.902	0.783	1.69	0.573	0.681	1.25	0.324	0.557	0.881
0.7	1.85	0.77	2.62	1.32	0.78	2.10	0.909	0.723	1.63	0.591	0.627	1.22	0.334	0.508	0.842
0.8	1.81	0.72	2.53	1.30	0.73	2.03	0.900	0.673	1.57	0.594	0.582	1.18	0.340	0.468	0.808
1.0	1.70	0.64	2.34	1.24	0.65	1.89	0.866	0.595	1.46	0.577	0.512	1.09	0.334	0.407	0.741
2.0	1.27	0.42	1.69	0.941	0.428	1.37	0.677	0.394	1.07	0.468	0.336	0.804	0.278	0.261	0.539
3.0	1.07	0.32	1.39	0.772	0.329	1.10	0.571	0.302	0.873	0.394	0.258	0.652	0.242	0.200	0.442
4.0	0.939	0.265	1.20	0.677	0.270	0.947	0.519	0.249	0.768	0.353	0.213	0.566	0.217	0.164	0.381
5.0	0.831	0.227	1.06	0.604	0.231	0.835	0.473	0.213	0.686	0.324	0.182	0.506	0.202	0.140	0.342
6.0	0.746	0.199	0.947	0.544	0.203	0.747	0.428	0.187	0.615	0.298	0.160	0.458	0.194	0.123	0.317

TABLE I. (*Continued.*)

E_p	Al^{5+}			Al^{6+}			Al^{7+}			Al^{8+}			Al^{9+}		
(MeV)	S_c	S_D	S_T	S_c	S_D	S_T	S_c	S_D	S_T	S_c	S_D	S_T	S_c	S_D	S_T
7.0	0.680	0.178	0.858	0.499	0.182	0.681	0.391	0.167	0.558	0.274	0.143	0.417	0.186	0.110	0.296
8.0	0.624	0.161	0.785	0.462	0.165	0.627	0.364	0.152	0.516	0.253	0.130	0.383	0.178	0.100	0.278
10.0	0.538	0.136	0.674	0.402	0.139	0.541	0.320	0.129	0.449	0.226	0.110	0.336	0.163	0.085	0.248
20.0	0.326	0.080	0.406	0.256	0.082	0.338	0.202	0.076	0.278	0.148	0.065	0.213	0.110	0.050	0.160
40.0	0.196	0.046	0.242	0.155	0.047	0.202	0.125	0.044	0.169	0.0948	0.0375	0.132	0.0717	0.0291	0.101
70.0	0.125	0.029	0.154	0.100	0.030	0.130	0.0808	0.0276	0.108	0.0619	0.0238	0.0857	0.0474	0.0185	0.0659
100.0	0.093	0.021	0.114	0.0742	0.0221	0.0963	0.0605	0.0205	0.0810	0.0466	0.0177	0.0643	0.0358	0.0137	0.0495

E_p	Al^{10+}			Al^{11+}		
(MeV)	S_c	S_D	S_T	S_c	S_D	S_T
0.1	0.007	0.619	0.626	0.00008	0.00063	0.00071
0.2	0.045	0.467	0.512	0.00056	0.00338	0.00394
0.3	0.085	0.388	0.473	0.00167	0.00733	0.00900
0.4	0.114	0.338	0.452	0.00345	0.0114	0.0149
0.5	0.134	0.302	0.436	0.00574	0.0152	0.0209
0.6	0.146	0.275	0.421	0.00838	0.0185	0.0269
0.7	0.153	0.253	0.406	0.0113	0.0213	0.0326
0.8	0.158	0.236	0.394	0.0143	0.0236	0.0379
1.0	0.163	0.209	0.372	0.0203	0.0271	0.0474
2.0	0.154	0.143	0.297	0.0439	0.0328	0.0767
3.0	0.143	0.113	0.256	0.0564	0.0321	0.0885
4.0	0.136	0.095	0.231	0.0624	0.0303	0.0927
5.0	0.128	0.083	0.211	0.0645	0.0284	0.0929
6.0	0.123	0.073	0.196	0.0641	0.0266	0.0907
7.0	0.119	0.066	0.185	0.0631	0.0249	0.0880
8.0	0.115	0.061	0.176	0.0616	0.0235	0.0851
10.0	0.106	0.052	0.158	0.0577	0.0211	0.0788
20.0	0.0739	0.0318	0.106	0.0421	0.0144	0.0565
40.0	0.0502	0.0189	0.0691	0.0307	0.0092	0.0399
70.0	0.0337	0.0122	0.0459	0.0212	0.0062	0.0274
100.0	0.0256	0.0091	0.0347	0.0162	0.0047	0.0209

TABLE II. For neutral Al, the calculated continuum S_c, discrete S_D, and total stopping power S_T (in 10^{-15} eV cm^2) subshell by subshell at 10 and 100 MeV. The Z^* values are the total subshell stopping powers normalized to 13. The Z^* values are compared with our summed oscillator strengths and those of Ref. 10 in the last two rows.

Subshell	1s	2s	2p	3s	3p	tot
			10 MeV			
S_c	0.0710	0.152	0.784	0.188	0.142	1.34
S_D	0.0003	0.002	0.004	0.144	0.062	0.212
S_T	0.0713	0.154	0.788	0.332	0.204	1.55
Z^*	0.60	1.29	6.61	2.78	1.71	13.0
$\sum f$ (present)	1.540	1.312	6.736	1.831	1.362	12.78
$\sum f$ (Ref. 10)	1.541	1.355	6.974	1.818	1.305	12.99
			100 MeV			
S_c	0.0209	0.0244	0.1140	0.0253	0.0184	0.203
S_D	0.0001	0.0003	0.0005	0.0185	0.0081	0.0275
S_T	0.0210	0.0247	0.1145	0.0438	0.0265	0.2305
Z^*	1.18	1.39	6.46	2.47	1.49	13.0
$\sum f$ (present)	1.540	1.312	6.736	1.831	1.362	12.78

$$E_{nl}^{\alpha_{nl}} S_{nl}^{C}(E_p) = g_{nl}\left[\frac{M_e E_p}{E_p E_{nl}}\right],$$

where α_{nl} approaches unity at high E_{nl} and $g_{nl}(\mu)$ is a scaling function. A plot of the maximum of S_{nl}^C multiplied by E_{nl} vs E_{nl} permitted the determination of α_{nl} and the range of E_{nl} to which it applied. Figure 1 shows such a plot for the 1s, 2s, and 2p subshells. The solid lines show the results for a large set of neutral-atom calculations. The open circles and crosses are results for the Al ions (with the Al results normalized to six 2p, and two 2s and 1s electrons). The scaled Al-ion results are in excellent agreement with the scaled neutral-atom results. This is a useful check on the calculated subshell stopping power near its peak, in contrast to the discussion in Sec. III which is limited to the asymptotic region.

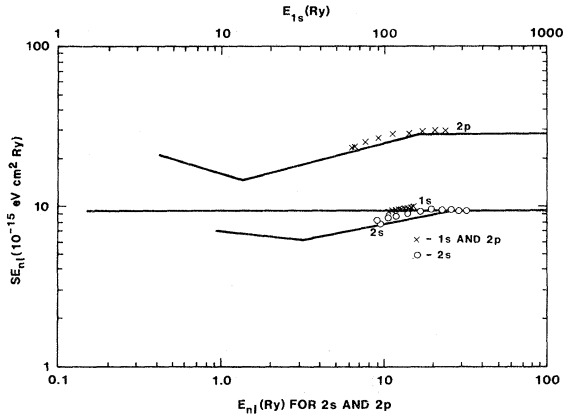

FIG. 1. Subshell-peak ionization stopping-power times subshell ionization energy vs subshell ionization energy for the 1s, 2s, and 2p subshells. The solid lines connect values obtained for neutral atoms. The unconnected points are Al-ion values.

III. THE ASYMPTOTIC REGION

The Bethe formula[8] gives the stopping power as

$$\frac{-1}{n}\frac{dE}{dx} = \frac{4\pi a_0^2 S(0)}{(M_e/M_p)E_p}\ln\left[\frac{4M_e}{M_p}\frac{E_p}{I}\right], \quad (4a)$$

with I determined by

$$\ln I = L(0)/S(0), \quad (4b)$$

with

$$L(0) = \sum_{nl,n'l'} f_{nl,n'l'}\ln[(E_{n'l'} - E_{nl})], \quad (4c)$$

$$S(0) = \sum_{nl,n'l'} f_{nl,n'l'} = \sum_{nl} S_{nl}(0), \quad (4d)$$

while $S(0) = \sum Z_{nl}$ is the Thomas-Reiche-Kuhn sum rule. In Eqs. (4) the summations include an integration over the continuum. From the explicit calculations, we evaluate I via

$$\sum_{nl}(S_{nl}^C + S_{nl}^D) = \frac{4\pi a_0^2(\sum Z_{nl})}{(M_e/M_p)E_p}\ln\left[\frac{4M_e}{M_p}\frac{E_p}{I}\right]. \quad (5)$$

Comparisons of Eqs. (4) and (5) indicate the

neglected transitions ($n' \geq 6$) will raise the I value as determined by Eq. (5) and may lower the I value determined by Eq. (4). As mentioned in Sec. II, excitations to levels with $n' \geq 6$ and $l' \geq 3$ were not included in the explicit stopping-power calculations. In evaluating $L(0)$ and $S(0)$ in Eq. (4), the missing discrete transitions were estimated from an n^{-3} scaling, using

$$f_{n_0 l, n' l'} = \frac{A}{(n')^3}(E_{n' l} - E_{n_0 l})$$

with A determined from the last excited level for which explicit calculations were performed. In calculating $L(0)$, $E_{n'l'}$ was set equal to zero for these transitions. Inclusion of the $n'l'$ levels with this estimate improved agreement with Thomas-Reiche-Kuhn sum rule, but did not change $\ln I$ by more than 1%. The changes in the summed oscillator strengths with the extrapolation was less than 2% for Al^{0+}, Al^{1+}, and Al^{2+}, rising to 7% at Al^{7+}, and falling to 3% at Al^{11+}. The use of the effective principal quantum number n^* rather than n, the principal quantum number, changed the $S(0)$ value by less than 1%; when the quantum defects $(n - n^*)$ were large (Al^{0+}, Al^{1+}, and Al^{2+}), the total correction was small. When the correction was larger, the quantum defects were small.

Table III compares some parameters in our calculation for neutral Al with the results of Dehmer *et al.*[10] and our integration of the photoabsorption cross section calculated by Reilman and Manson.[11] Our integrated continuum oscillator strength is closer to that of Reilman and Manson[11] than of Dehmer *et al.*[10] The last row in Table II compares our calculated subshell $\sum f$ values with adjusted[12] values of Dehmer *et al.*[10] Our overall $\sum f$ (12.78) differs from the expected sum-rule value by 0.22 or 1.7%. Comparison with the results of Dehmer *et al.*[10] suggests that the missing oscillator strength is in the $2p$ subshell. It is likely that the departure of our calculated total oscillator strength from the sum-rule value arises from our use in calculating oscillator strengths of an energy grid less than optimum for sum-rule evaluation.

TABLE III. Comparisons of our summed oscillator strengths and mean-excitation energy for neutral Al and those of Refs. 10 and 11. The I value in parenthesis is obtained with $S(0)=13.0$, while the first entry uses $S(0)=12.78$.

	$\sum fn$	$\int \frac{df}{d\epsilon} d\epsilon$	$S(0)$	$L(0)$	I(eV)
Present	2.444	10.333	12.78	28.12	122.8(118.3)
Reference 10	2.35	10.65	13.0	28.76	124.3
Reference 11		10.41			

Because our summed oscillator strength does not satisfy the sum rule, there is an ambiguity in the choice of the number of bound electrons or $\sum f$ for $S(0)$ in the determination of I via Eq. (4). In Tables III and IV we show I determined with $\sum f$ and in parenthesis I determined by the number of bound electrons. From Table III it is clear that for neutral Al, either choice leads to good agreement with the value of Dehmer *et al.*[10]

In Table IV we list $S(0)$, $L(0)$, and I calculated via Eq. (4) with our optical oscillator strengths for Al ions[13] Except for neutral Al, $S(0)$ is slightly larger ($\leq 2\%$) than the sum-rule value. Also listed are the I values calculated via Eq. (5) using the 10 and 100 MeV results of Table I. Even at 100 MeV, I values calculated via Eq. (5) can be 50% larger than I

TABLE IV. Summed oscillator strengths and mean-excitation energies from Eq. (4a) for Al ions. Columns 6 and 7 are I values at 10 and 100 MeV obtained from Eq. (5) and the calculations in Table I. Column 9 is an $L(0)$ value obtained from the calculations in Table I at 100 MeV.

Al^{n+}	$S(0)$	$L(0)$	I(eV)		I(eV)/10 MeV	I(eV)/100 MeV	% difference	$L'(0)$	% difference
0	12.78	28.12	122.8	(118.3)	142.2	120.7	−1.7	28.38	0.92
1	12.06	29.73	160.0	(162.0)	189.0	172.9	8.1	30.51	−2.6
2	11.11	31.11	223.7	(230.0)	308.2	264.5	18.2	32.65	−5.0
3	10.13	31.70	310.9	(323.8)	433.9	372.2	19.7	33.09	−4.4
4	9.155	29.07	325.5	(343.8)	476.8	426.4	31.0	31.01	−6.7
5	8.162	27.40	390.4	(417.8)	622.5	532.8	36.5	29.34	−7.1
6	7.148	25.13	457.5	(492.8)	835.0	656.0	43.4	27.13	−8.0
7	6.124	22.44	530.8	(572.5)	926.3	731.1	37.7	23.91	−6.6
8	5.018	19.35	643.0	(652.0)	1279.0	957.8	49.0	21.27	−9.9
9	4.057	16.62	817.9	(867.0)	1592.0	1175.0	43.7	17.84	−7.3
10	3.029	13.66	1236.0	(1291)	2360.0	1653.0	33.7	14.40	−5.4
11	2.007	10.36	2373.0	(2416)	4132.0	2677.0	11.4	10.56	−1.9

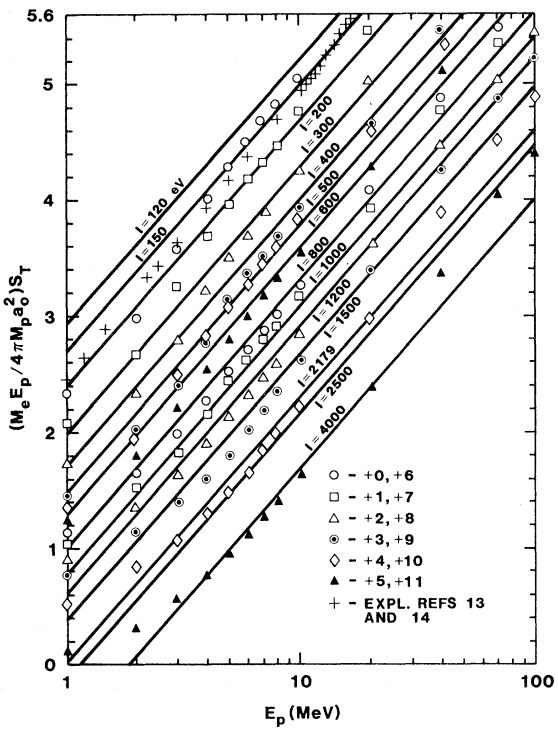

FIG. 2. Fano plot for the Al-ion calculations between 1.0 and 100 MeV. The crosses are experimental points from Refs. 13 and 14.

values calculated via Eq. (4). I values calculated at 10 MeV via Eq. (5) can be a factor of 2 larger than I values calculated via Eq. (4). Column 8 in Table IV shows the percent differences in $(I-I_{100\text{ MeV}})/I$. Column 9 lists an effective $L(0)$ $[L'(0)]$ obtained from Eq. (4b) using the I value obtained from the explicit calculations at 100 MeV. The percent difference between this $L'(0)$ and the $L(0)$ from Eq. (4) is shown in the last column. This percent difference measures the difference between the stopping power calculated explicitly and via the Bethe formula at 100 MeV, i.e., they agree to better than 10%.

To illustrate the departure of the explicitly calculated stopping powers from the Bethe formula, Fig. 2 shows the calculations in a Fano plot.[14] That is, we plot

$$\frac{M_e E_p}{M_p 4\pi a_0^2 S(0)}\left[\sum_n S_{nl}^C + S_{nl}^D\right]$$

vs $\ln E_p$ as points for the ions indicated and show $\ln(4M_e E_p/M_p I)$ vs $\ln E_p$ as solid lines for a variety of I values. Also plotted in Fig. 2 are the measurements of Luomajärvi[15] for (1.0—1.5)-MeV protons and Sorensen and Andersen[16] for (2.25—18)-MeV protons (shown as crosses).[17] The calculated stopping power and experimental measurements on solid Al shown in Fig. 2 have a maximum difference of 10% above 1 MeV. Because of the difficulties in extracting accurate I values from total-stopping-power data, demonstrated in part by the preceding discussion of our theoretical data, we do not here present a comparison between theory and experiment. One of us will do so elsewhere.[18]

For neutral Al the explicit calculations show a rise on the modified Fano plot between 2 and 4 MeV. The experimental data show a more gradual rise. This change on the Fano plot is due to ionization of the 1s subshell. The lowest set of explicit calculations, Al^{+11}, shows a rise between 20 and 40 MeV. This is due to our treatment of the asymptotic Bethe ridge, i.e., the region of the GOS that we approximate by $Z\delta(\epsilon-K^2)$ for the 1s subshell. This region of the GOS contributes about 10% of the calculated stopping power of Al^{11+} at 100 MeV.

IV. CONCLUSIONS

These calculations for the proton stopping power of Al ions will be applied to systems where there are no experimental data to check their validity. For neutral Al above 1 MeV, the calculations have been shown to agree with experiment on solid Al to better than 10%. The stopping powers are based on GOS calculations. The GOS have been used to calculate electron ionization cross sections and these are in good agreement with available measurements and other calculations.

A comparison of subshell-peak ionization stopping power for the 1s, 2s, and 2p subshells show these results to be in excellent agreement with scaled atomic subshell-peak ionization stopping powers. A comparison of Bethe mean-excitation energies, calculated using calculated optical oscillator strengths with I values inferred from the explicit stopping-power calculations at 100 MeV, showed differences of as much as 50% through the stopping powers themeselves differed by less than 10%. Consequently, we estimate that the stopping powers given in Table I are accurate to better than 20%.

ACKNOWLEDGMENT

This work was supported by the United States Department of Energy.

[1]D. J. Johnson, G. W. Kuswa, A. V. Farnsworth, Jr., J. P. Quintenz, R. J. Leeper, E. J. T. Burns, and S. Humphries, Jr., Phys. Rev. Lett. 42, 610 (1979).

[2]I. Yu. Skobelev, A. V. Vinogradov, and E. A. Yukov, Phys. Scr. 18, 78 (1978).

[3]L. E. Chase, W. C. Jordan, J. D. Perez, and J. G. Pronko, Appl. Phys. Lett. 30, 137 (1977).

[4]E. J. McGuire, Phys. Rev. A (in press).

[5]E. J. McGuire, Phys. Rev. A (in press).

[6]F. Herman and S. Skillman, *Atomic Structure Calculations,* (Prentice-Hall, Englewood Cliffs, N.J., 1963).

[7]E. J. McGuire, Phys. Rev. A 26, 125 (1982).

[8]H. A. Bethe, Ann. Phys. (Leipzig) 5, 325 (1930); Z. Phys. 76, 293 (1932).

[9]E. J. McGuire, Phys. Rev. A 16, 62 (1977).

[10]J. L. Dehmer, M. Inokuti, and R. P. Saxon, Phys. Rev. A 12. 102 (1975).

[11]R. F. Reilman and S. T. Manson, Astrophys. J. Suppl. 40, 815 (1979).

[12]The worksheets kindly provided to one of the authors (J.M.P.) by Dr. Inokuti show an anomalous $\sum f$ for the 1*s* subshell of Al($\sum f=1.451$), which also appears in Fig. 7 of Ref. 10. This lowers their summed oscillator strength to 12.90. Assuming an interchange of digits, (i.e., $\sum f=1.541$ for the 1*s* subshell) removes the anomaly, brings the overall sum to 12.99, and is in excellent agreement with our calculated $\sum f$ value for the 1*s* subshell.

[13]A comparison of these I values with those obtained from alternative techniques can be found in a forthcoming publication [J.M. Peek, Phys. Rev. A 26, 1030 (1982).]

[14]U. Fano, Phys. Rev. 95, 1198 (1954).

[15]M. Luomajarvi, Rad. Eff. 40, 173 (1979).

[16]H. Sorensen and H. H. Andersen, Phys. Rev. B 8, 1854 (1973).

[17]Our calculations are nonrelativistic. The data include relativistic effects approximately given by $\ln[1/(1-\beta^2)]-\beta^2$ which is 0.001 for 20-MeV protons and is a negligible correction to the nonrelativistic stopping power at this energy.

[18]E. J. McGuire, Phys. Rev. A (in press).